CellPress

Developmental Cell
Review

The Canonical Notch Signaling Pathway: Structural and Biochemical Insights into Shape, Sugar, and Force

Rhett A. Kovall,[1,*] Brian Gebelein,[2] David Sprinzak,[3] and Raphael Kopan[2,*]
[1]Department of Molecular Genetics, Biochemistry and Microbiology, University of Cincinnati College of Medicine, Cincinnati, OH 45267, USA
[2]Division of Developmental Biology, Children's Hospital Medical Center, Cincinnati, OH 45229, USA
[3]Department of Biochemistry and Molecular Biology, The George S. Wise Faculty of Life Sciences, Tel Aviv University, Tel Aviv 69978, Israel
*Correspondence: kovallra@ucmail.uc.edu (R.A.K.), raphael.kopan@cchmc.org (R.K.)
http://dx.doi.org/10.1016/j.devcel.2017.04.001

The Notch signaling pathway relies on a proteolytic cascade to release its transcriptionally active intracellular domain, on force to unfold a protective domain and permit proteolysis, on extracellular domain glycosylation to tune the forces exerted by endocytosed ligands, and on a motley crew of nuclear proteins, chromatin modifiers, ubiquitin ligases, and a few kinases to regulate activity and half-life. Herein we provide a review of recent molecular insights into how Notch signals are triggered and how cell shape affects these events, and we use the new insights to illuminate a few perplexing observations.

At its core, Notch signaling involves: (1) cell-to-cell contacts that enable Notch receptor and Delta/Serrate/Jagged ligand (henceforth DSL) interactions; (2) a receptor-ligand force generation system that unfolds a protective domain within the Notch receptor (the negative regulatory region [NRR]) to thereby allow sequential proteolytic activation and release of the Notch intracellular domain (NICD); and (3) NICD translocation from membrane to nucleus where it binds a conserved transcription factor (CSL; CBF1/RBPJ, Su(H), Lag-1) to upregulate Notch target genes. A previous mechanistic review (Kopan and Ilagan, 2009) described the core components, suggested how ligand/receptor interactions promote the proteolytic activation mechanism, described the structural insights available at the time, and detailed the nuclear exploits of NICD, RBPJ, and their associated proteins. Sufficient progress has been made in all these areas to warrant crafting an update. Herein, we will update the reader on structure-based insights into Notch receptor/ligand interactions, the proteins involved in receptor modifications and cleavage, the details on what forces are required to activate Notch and how cell shape might effect this process, and end by updating the reader on how the active NICD molecule mediates changes in gene expression. We aim to provide a more in-depth discussion of selected studies and supplement rather than replace the previous work (for recent comprehensive reviews, see Aster et al., 2017; Bray, 2016). As was done in the original review, we organized the information in a manner reflecting the flow of information in the Notch signaling pathway: from the outside in.

Structural Biology Illuminates Receptor-Ligand Interactions at the Cell Surface

A mechanistic understanding of Notch signaling requires the elucidation of how receptor-ligand interactions unfold the NRR to promote proteolytic cleavage within the membrane. Several technical hurdles had to be overcome to address this problem, including the size and complexity of the extracellular domains (ECDs) of ligand and receptors, their relatively weak affinity to each other, and the extreme lipophilic nature of γ-secretase, all of which impeded detailed analyses of the receptor/ligand/protease complexes at the atomic level. Recent technological advances such as in vitro evolution binding assays and cryoelectron microscopy (cryo-EM) have begun to overcome these obstacles. In this section, we highlight new findings that provide insight into how the ligand and receptors interact, the role of glycan modifications in these interactions, the range of forces involved and how they are generated, and, finally, the machinery that cleaves the Notch receptor to release NICD.

Rod or Nunchaku?

The ECDs of Notch receptors and DSL ligands are largely composed of multiple iterative EGF repeats (mammalian Notch receptors have 29–36 repeats [Figure 1], whereas DSL ligands vary in EGF repeats from 6 to 16; D'Souza et al., 2010; Kopan and Ilagan, 2009). Both the DSL domain and the EGF repeats are small ~40 residue modular domains that are primarily composed of β strands and contain three conserved disulfide bonds. Prior structures of 3 EGF repeats from either human Notch1 or Jag1 revealed an elongated rod-like architecture (Cordle et al., 2008; Hambleton et al., 2004), which supported the interpretation that the ECD of Notch and DSL ligands would assume a largely elongated, rigid linear topology at the cell surface. However, recent structural and biophysical studies of Notch receptors and DSL ligands point to a structure of multiple rods connected by flexible joints. This architecture most likely contributes to function.

It was thought that the DSL domain within each ligand interacted with Notch EGF11-12, with possible involvement of additional domains (Kopan and Ilagan, 2009). Kershaw et al. (2015) solved the X-ray structure of the entire ECD of human DLL1, which contained the MNNL (module at the N terminus of notch ligands) and DSL domains, and EGF repeats 1–8 (note that EGF7-8 were not visible in the structure) (Figure 1). MNNL is a C2 domain, which has a β sandwich fold and is often involved in binding of phospholipids (Chillakuri et al., 2013), whereas DSL is a small ~40 residue domain composed of β strands, analogous to EGF repeats. Overall, DLL1 assumes an extended

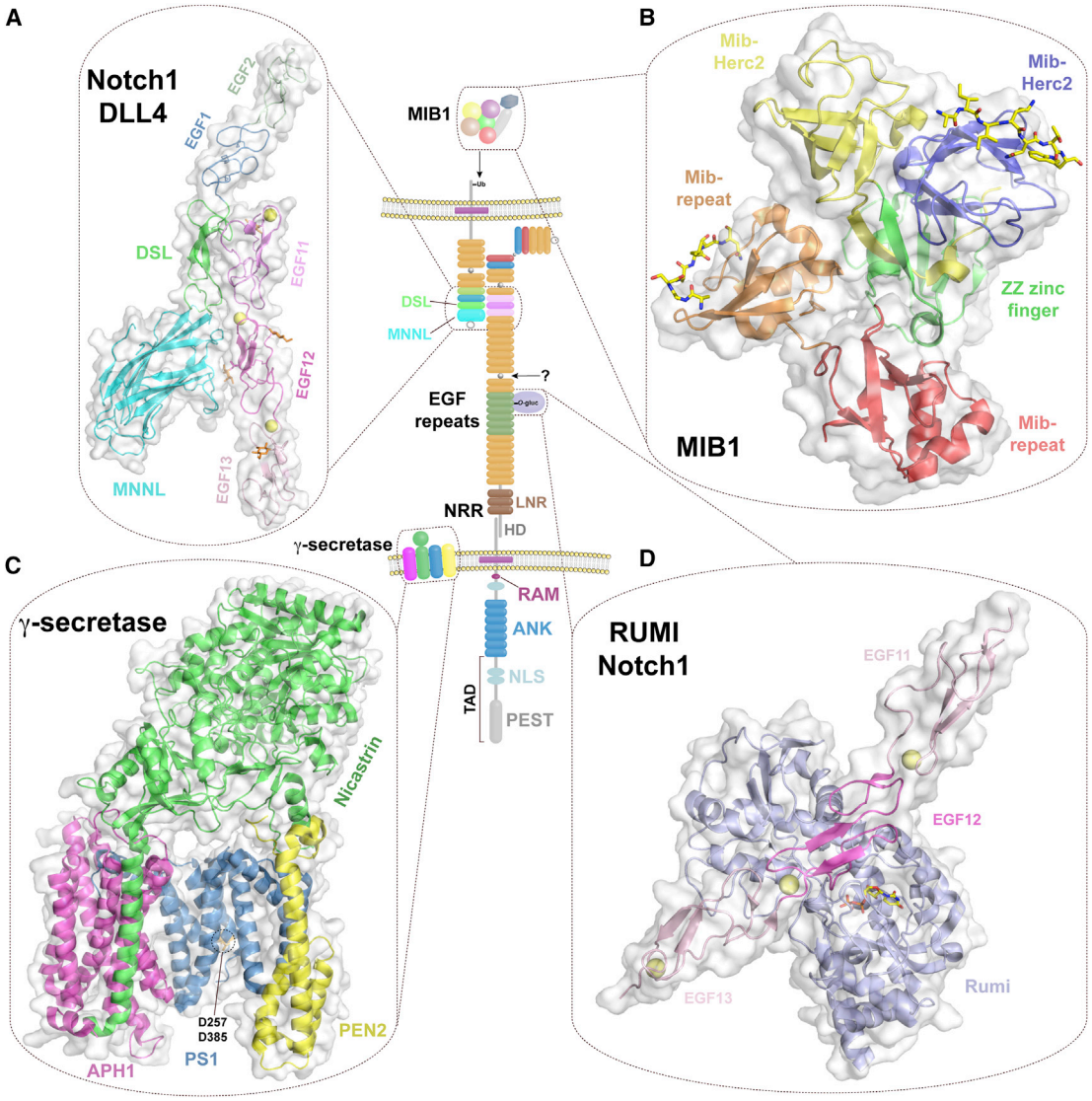

Figure 1. Domain Schematics and Their Structure and Other Structural Insights

The central figure shows domain organization of a Notch receptor and a DLL ligand, γ-secretase, and Mib-1. The extracellular domain of Notch receptors (*Notch1 shown*) consists of multiple iterative EGF repeats followed by the NRR (negative regulatory region), which consists of three LNR (Lin-12 and Notch repeats) domains and HD (heterodimerization domain). EGF repeats for which no structure was determined are colored orange or green (representing the location of Abruptex alleles). EGF repeats in any other color denote recent structure determinations. There is a ~90° bend between EGF5-6, as well as a flexible joint between EGF9-10; mobility near EGF22 is yet to be determined. The intracellular domain of Notch receptors consists of a membrane proximal RAM (RBPJ associated molecule) domain, ANK (ankyrin repeats), and a C-terminal TAD (*trans*-activation domain) comprised of three NLS (nuclear localization sequences) and degron-containing PEST (*for rich in* proline, glutamate, serine, and threonine) sequence. The extracellular domain of DSL ligands (DLL4 shown) consists of an N-terminal MNNL (module at the N terminus of Notch ligands) domain, DSL domain, and additional EGF repeats with a potential flexible joint between EGF4-5.

(A) X-ray structure of the Notch1-DLL4 complex (PDB: 4XLW). All domains in the crystal are colored as in the diagram, bound Ca^{2+} ions are shown as yellow spheres, and glycan modifications are shown in a stick representation and colored orange.

(B) X-ray structure of Mib1 (PDB: 4XI6). Mib1 is composed of two N-terminal Mib-Herc2 domains, colored yellow and purple, with a ZZ zinc-finger domain (green) in between them. These are followed by two Mib-repeat domain colored orange and red. The Jagged1 N-box peptide bound to the first Mib-Herc2 domain (purple) is shown in a stick representation. The modeled C-box peptide bound to the first Mib-repeat (orange) is also shown in a stick representation with carbon, oxygen, and nitrogen atoms colored yellow, red, and blue, respectively.

(C) High resolution cryo-EM structure of the γ-secretase complex (PDB: 5A63). The Nicastrin, Aph-1, PS1, and Pen-2 subunits are colored green, magenta, blue, and yellow, respectively. Note that catalytic aspartates (D257 and D385) in PS1 are not facing the cavity.

(D) X-ray structure of Rumi (PDB: 5F84) modeled with EGF11-13 from Notch1. Rumi is colored light blue and EGF11-13 are colored pink/magenta. Bound UDP moiety is shown in stick representation with carbon, oxygen, and nitrogen atoms colored yellow, red, and blue, respectively.

conformation that is largely linear from the MNNL through the first 4 EGF repeats, measuring ~195 Å along its longest axis. Overlay of this region with the structure of Jag1 (Chillakuri et al., 2013) suggests that all DSL ligands adopt a similar conformation. Strikingly, the DLL1 structure reveals a 90° turn at the junction between EGF4,5 with EGF5,6, resuming a linear

conformation. Given that this region of the structure is involved in crystal lattice contacts, the authors suggest that a range of bend angles may be accommodated between these repeats; however, this remains to be experimentally determined. The residues at the distinct bend are well resolved in the structure, and are conserved in other ligands, suggesting that the bend observed in DLL1 is also conserved in other DSL molecules.

The ECD of Notch receptors contains two types of EGF repeats: Ca^{2+} binders and non-binders. Previous studies of the ligand-binding region of Notch1 (EGF11-13) showed that all three repeats bind Ca^{2+} and assume a near linear and rigid conformation (Hambleton et al., 2004). To assess the flexibility between the other EGF repeats that compose the Notch ECD, the Handford and Redfield groups used nuclear magnetic resonance (NMR) spectroscopy, X-ray crystallography, and biochemical/cellular binding assays to analyze the conformations of the EGF repeats derived from EGF4-13 of human Notch1 (Weisshuhn et al., 2016). They found that Ca^{2+} binding by repeats 5, 7, 8, 9, 11, 12, and 13 occurs in the micromolar range, consistent with these sites being largely occupied under physiological conditions of Ca^{2+} (1.4 mM). However, X-ray structures of EGF repeats 4–7 from human Notch1 (Weisshuhn et al., 2015a) show a striking tilt angle of ~90° between repeats 5 and 6, which do not bind Ca^{2+} (Figure 1). To analyze additional tilt/twist angles between EGF repeats, the authors used NMR spectroscopy with constructs corresponding to Notch1 EGF repeats 4–7, 7–9, 8–11, and 11–13 (Weisshuhn et al., 2015b). These studies confirmed that Ca^{2+} binding EGF repeats assume a rigid rod-like structure. EGF repeats 4–5, 6–7, 11–12, and 12–13 have modest tilt angles, ranging from ~16° to 48°. These NMR data are consistent with the tilt angles observed in the X-ray structures of EGF repeats 4–7 and 11–13. Interestingly, interspersed between these rigid rods are EGF6, 10, and 22, which do not contain the Ca^{2+} binding consensus sequence of D/N-x-D/N-E/Q-xm-D/N-xn-Y/F and therefore may act as flexible joints within the Notch1 ECD. Accordingly, NMR data demonstrate that the linkage between EGF repeats 5–6 has the largest tilt angle (~70°), and the linkage between EGF repeats 9–10 is flexible. Based on these results, the authors constructed an informed model of EGF repeats 4–13 of hNotch1, which consists of a flexible region between EGF repeats 9–10 separating two rigid segments between repeats 4–9 and 10–13. EGF repeats 4–9 take on an "L shape" conformation due to the bend between repeats 5–6, with repeats 10–13 assuming a more linear arrangement, albeit with a modest bend between repeats 10–11 (Figure 1).

Receptor-Ligand Complexes Studied at the Atomic Level

In addition to studies on the isolated ECDs of receptor and ligand, two landmark studies by the Garcia group solved the X-ray structures of Notch1-DLL4 (Luca et al., 2015) and Notch1-Jag1 complexes (Luca et al., 2017). To overcome the inherent low affinity between ligand and receptor in solution, Luca et al. used an in vitro evolution procedure to identify ligand mutations that increased their affinity for the receptor to permit crystallization. Interestingly, the stabilizing variants map to regions outside the Notch-DSL interface; one possibility is that the mutations increase the stability and/or rigidity of the ligand, thereby indirectly increasing the affinity of the receptor-ligand complex; another possibility is that the mutations increase the propensity of the ligand to adopt a high-affinity conformation for the receptor. Nonetheless, this enabled the structural details of how Notch receptors interact with ligands and the role glycosylation plays in modulating this interaction. Previous models proposed both parallel and antiparallel orientations between ligand and receptor (Cordle et al., 2008), whereas the structures show that both the MNNL and DSL domains of DLL4 and Jag1 interact with EGF12 and 11 of Notch1 in an antiparallel fashion. Moreover, the authors suggest that an antiparallel orientation is consistent with both *trans*-activation and *cis*-inhibition if the flexibility of these large, multi-EGF repeat-containing ECDs are taken into account. Interestingly, the "synNotch" proteins (Morsut et al., 2016) also recapitulate *cis*-inhibition, reinforcing the argument that the binding modes for activation and inhibition are very likely to be the same.

Using the new data of Notch/DLL4 interactions, Weisshuhn et al. (2016) performed an in silico structural overlay of their Notch1 EGF10-13 structure with EGF11-13 from the Luca et al. complex. They uncovered a potential interaction between EGF10 in Notch1 with EGF1 of DLL4. Using a cell-based flow cytometry assay, Weisshuhn et al. (2016) were able to show that inclusion of EGF10 from Notch1 decreased binding to full-length DLL4; however, addition of EGF9 resulted in no further reduction in Notch1/Dll4 interactions. Interestingly, the addition of EGF10 had no effect on the interactions between Jag1 and Notch1, beginning to differentiate the interaction interfaces between Notch1 and its two ligand families.

Comparison between the receptor-ligand complexes reveals that the interface between Notch1 and DLL4 is larger than the interface between Notch1 and Jag1. This is consistent with DLL4 having a higher in vitro affinity for Notch1 than Jag1 (Andrawes et al., 2013). Interestingly, whereas Notch1-DLL4 interactions involve only EGF10-13, the Notch1-Jag1 complex structure (Luca et al., 2017) shows that EGF1-3 in Jag1 makes additional interactions with EGF8-10 in Notch, as predicted by genetic studies in flies showing that Notch EGF8 mediates Serrate-specific interactions (Yamamoto et al., 2012). This observation led the authors to speculate that the Notch1-Jag1 interaction resemble *catch bonds* in which the strength of interaction is increased when greater forces are applied or when sheer stress is present. Using biomembrane force probe force-clamp spectroscopy, Luca et al. showed that, indeed, the Notch1-Jag1 interaction involves catch bonds, but the Notch1-DLL4 complex does not. This finding suggests that when a low force is applied, the Jag/Notch interaction may be unproductive (i.e., without NRR unfolding), whereas Dll4/Notch1 interactions under similar force result in receptor activation. However, increasing the force will trigger Jag1/Notch1 activation. This difference may be important for the function of distinct ligands under different physiological settings. For example, during angiogenesis a new endothelial cell phenotype is formed in response to vascular endothelial growth factor (VEGF) signals from the environment, called a tip cell (Benedito et al., 2009). The tip cell moves toward the source of VEGF signaling to the trailing cell via Dll4, activating Notch1, which inhibits VEGF receptor expression and thus reinforces a trailing stalk cell morphology and function on the signal-receiving cell. The stalk cell expresses Jag1, which binds Notch1 and sequesters it from Dll4 without activating it, tuning the number of productive receptor/ligand interactions and, thus, the number of tip cells

(Benedito et al., 2009). The inability of Jag1 to activate Notch1 in this system can potentially be attributed to the lower force applied (see the following section). In contrast, the shear stress that results from blood flow may potentiate Notch/Jag interactions between the endothelial cells lining the vessels, where Notch1 activation by Jag1 is critical for preventing aortic valve calcification (Garg et al., 2005; Theodoris et al., 2015).

Some Notch Receptors Are Sweeter than Others

Another front where significant progress has been made in recent years is the role of Notch glycosylation. It was known that ECD glycosylation is essential for Notch signaling in some cellular contexts, and can profoundly modulate signaling between different receptor-ligand pairs in other contexts (Stanley and Okajima, 2010). However, the exact role of glycosylation at the receptor/ligand interface was unclear and not all of the enzymes involved in receptor/ligand modifications were identified in 2009. To date, known modifications of EGF repeats in the Notch ECD include O-fucosylation, O-glucosylation, and O-GlcNAcylation by the enzymes POFUT1, POGLUT1, and EOGT1, respectively. O-Fucose modifications of Notch can be extended by the Fringe family of GlcNAc-transferases and O-glucose can be extended by the xylosyltransferases GXYLT1/2 and XXYLT1 (Lee et al., 2013; Sethi et al., 2010, 2012). As predicted by the impact of removing Thr466 from EGF12 of Notch1 (Ge and Stanley, 2008), the fucose at this residue anchors the interaction with MNNL (Luca et al., 2015). Modeling of the disaccharide formed by the extension of O-fucose at Thr466 by Fringe suggested that additional interactions could form with the MNNL, providing a structural rationale for how glycan modifications can increase the affinity of some ligands for the Notch receptor (Luca et al., 2015). Unexpectedly, the O-glycan modification at Ser435 in Notch1 (EGF11, Andrawes et al., 2013), also makes interactions with the DSL domain (Luca et al., 2015). The functional consequence of glycosylation at this position remains to be determined, as is the identity of the enzyme responsible.

Recent advances elucidate in more detail the extent EGF repeats are modified, and the structural basis for how glycosyltransferases recognize and modify specific repeats. Using semi-quantitative mass spectrometry methods, the Haltiwanger group published a comprehensive study mapping glycan modifications of the Notch receptor in *Drosophila* S2 cells in the presence or absence of Fringe (Harvey et al., 2016). The ECDs of *Drosophila* Notch has 36 EGF repeats, each composed of approximately 40 residues with three disulfide bonds. Based on consensus sequences, Notch is predicted to have 22 O-fucose, 18 O-glucose, and 18 O-GlcNac sites. Harvey et al. showed that the majority of O-fucose sites were modified efficiently; however, Fringe only extended a subset of these sites to disaccharides. Similarly, Rumi, the *Drosophila* POGLUT1 ortholog, efficiently modified all O-glucose consensus sites with only a fraction of these sites containing di- and trisaccharide modifications. Of the potential 18 O-GlcNac sites in Notch, only five showed any appreciable modification. Harvey et al. also showed that Notch purified from *Drosophila* embryos had levels of O-glycosylation similar to those in S2 cells. Thus, individual Notch molecules are differentially modified, and this local heterogeneity would impact the likelihood that an individual receptor/ligand interaction will result in NICD release. Kakuda and Haltiwanger (2017) extended these observations to a mammalian Notch protein, establishing that Lunatic and Manic Fringe modified similar sites on Notch1, including those at EGF8 and 12. Interestingly, modifications at EGF6 and 36 (added by Manic and Lunatic, but not Radical Fringe) specifically inhibited Notch1 activation by Jagged1. How modifications of a residue on EGF36 can inhibit Jag1-mediated activation is currently a mystery. Combined, these conclusions could explain why only a small fraction of the cellular receptor pool undergoes cleavage, and the presence of specific Fringe enzymes could help to fine-tune the response of Notch receptors to available ligands in different cellular environments.

Glycosyltransferase Crystalized

Importantly, glycosylation may become therapeutically exploitable to tune signaling levels. To that end, some structural insights into the enzymes glycosylating Notch have been uncovered (Figure 1). Yu et al. (2015, 2016) solved X-ray structures of the endoplasmic reticulum (ER) enzyme xyloside α-1,3-xylosyltransferase (XXYLT1), a well-conserved type II membrane protein that can extend O-glucose modifications within Notch EGF repeats. In addition they solved the structure of Rumi alone and in complex with an EGF repeat derived from the coagulation factor IX containing a Xyl-Glc disaccharide modification. These structures provided mechanistic insights into how these enzymes bind to and modify Notch. In the apo structure (the enzyme without a substrate), XXYLT1 forms a dimer such that the enzyme active sites are in an ideal conformation to interact with laterally oriented Notch EGF repeats within the ER lumen (Yu et al., 2015). The structure of XXYLT1 is largely unchanged when in complex with the EGF repeat, but, unexpectedly, the structure of the EGF repeat undergoes a large conformational change while maintaining all disulfide bonds. The two β strands of the EGF repeat assume a more extended conformation, suggesting that EGF repeats have more structural flexibility than previously thought. Using the factor IX EGF/XXYLT1 structure as a guide, the authors docked the EGF repeats 11–13 from Notch1 in silico, which revealed that the N-terminal repeats of Notch would be oriented away from the luminal membrane, whereas the C-terminal repeats would face toward the membrane.

Rumi/POGLUT1 is the glycosyltransferase that adds O-glucose moieties to serine residues within EGF repeats containing the consensus sequence C-X-S-X-(P/A)-C. The structure shows that Rumi is composed of two domains with $\beta\alpha\beta$ folds (Rossmann fold), in which the EGF repeat binds within a cleft between the two domains (Yu et al., 2016) (Figure 1). The O-glucosylation consensus sequence C-X-S-X-(P/A)-C forms a U-shaped structural motif. Unexpectedly, Rumi also interacts with a previously unknown hydrophobic region in the EGF repeat through a region conserved in Rumi orthologs. In contrast to the XXYLT1-EGF structure, neither Rumi nor its bound EGF repeat undergo any appreciable conformational changes upon complex formation.

Finally, Lira-Navarrete et al. (2011) solved the X-ray structure of POFUT1 from *C. elegans* alone and in complex with guanosine diphosphate (GDP) and GDP-fucose. POFUT1 fucosylates serine/threonine residues present in the EGF repeats of Notch receptors, containing the consensus sequence C-X(4–5)-[S/T]-C, which can be further modified with GlcNAc by Fringe proteins. Similar to POGLUT1, POFUT1 is also a two-domain protein with $\beta\alpha\beta$ folds. The authors modeled EGF12 from Notch1

into the active site of POFUT1, noting excellent complementarity between the two structures and reasonable proximity between GDP-fucose in the POFUT1 active site and the modified threonine residue in Notch.

Mechanotransduction of Notch Activation

Although the concept of a pulling force required for Notch activation has been around for nearly two decades (Kopan and Ilagan, 2009; Parks et al., 2000); however, only recently have studies employed molecular force measurements to test this hypothesis and directly measure the forces required for activating ligand-receptor pairs. A first attempt to measure the forces required for Notch receptor activation was performed by Wang and Ha (2013). To measure the force, they used double-stranded DNA molecules as tension gauge tethers (TGT) designed to sustain a defined level of tension before breaking apart. By presenting cell lines containing a Notch-Gal4 reporter onto a plate-bound TGT attached to the Dll1-ECD, they demonstrated that forces as low as 12pN could trigger Notch proteolysis and reporter activation. Interestingly, the force required for activation of Notch is significantly smaller than the force required for separating the ligand-receptor pair (19 pN; Shergill et al., 2012). Recently, the Ha group revisited the force requirements with an improved approach (termed low TGT or LTGT) allowing them to map activation forces to a value between 4 and 12 pN (Chowdhury et al., 2016).

Independently, Gordon et al. (2015) used another clever setup to measure activation forces. By varying the distance between samples and a fixed magnetic field, they applied pulling forces to either a plate-tethered NRR domain or to Notch receptors expressed in live cells. In their assay, forces as small as 4–5 pN were sufficient to enable cleavage of the NRR domain by ADAM17, or to induce the activation of Notch receptors in live cells. Furthermore, they show that force-induced signals can be triggered even when the EGF repeats in the receptors and ligands are replaced by a synthetic FKBP-FRB binding domain. This result established that the pulling force needed to unfold the NRR can be applied directly to this domain, and indirectly argued that allosteric interactions mediated by EGF repeats are not needed: a force on the order of 5 pN is both necessary and sufficient for NRR unfolding and for Notch activation. It is important to note here that ADAM10, and not ADAM17, is involved in activation of Notch receptor by their ligands in living cells. The preferential activation of EDTA-unfolded NRR by ADAM17 in cell culture reflects differential sensitivity to the inhibitory effect of EDTA: ADAM10 is inhibited, whereas ADAM17 is not (Blobel, C., personal communication; Groot et al., 2013).

More recently, Seo et al. (2016) refined the use of magnets to test the requirement of pulling force at the single-molecule level in live cells. They used SNAP-tag chemistry to monovalently link engineered Notch receptors (fused to mCherry) to magnetoplasmonic nanoparticles (MPNs). This approach allowed pulling on single beads, each attached to one receptor. Maneuvering a magnetic atomic force microscope tip toward the cell surface modulated the pulling force. The authors showed that at low force (1 pN) they could cluster Notch receptors and move them around as they followed the tip, but the intracellular mCherry was not released, indicating that the NRR, and thus the receptors, remained intact. In contrast, pulling Notch receptors at a single spot with 9 pN force was sufficient to induce a release of mCherry. Next, they asked if clustering of receptors or if complexing endogenous Notch with MPN conjugated to Dll1-ECD (single- or multivalent Dll1-MPNs) could lead to activation at 1 pN. They concluded that neither clustering nor binding of the ligand are sufficient to activate Notch, arguing again that allostery is not required, nor does it facilitate, NRR unfolding. Collectively, these experiments agree that forces between 4 and 9 pN are sufficient to unfold the Notch1 NRR in response to Dll1, and demonstrate that the ECD of Notch and Dll1 does not impact the magnitude of forces needed to directly fold an NRR coupled to synthetic ligands.

While the force measurement experiments show that a 4–9 pN force is sufficient to activate Notch, the identity of the in vivo force generators that mediate receptor activation remain poorly defined. It has long been suspected that ligand endocytosis can serve as a pulling-force generator on the ligand side. However, it was unclear whether the forces generated by ligand endocytosis are within the 4–9 pN range. Weinmaster and her colleagues (Meloty-Kapella et al., 2012; Shergill et al., 2012) demonstrated that epsin- and clathrin-mediated endocytosis generated sufficient force to activate Notch signals in vivo and in vitro (Meloty-Kapella et al., 2012). Using N1-Fc tethered to beads and optical tweezers they measured the endocytic pulling forces exerted by Dll1-expressing cells. The forces averaged around ~3 pN, but reached up to 10 pN, consistent with the pulling forces required for Notch activation for some, but not all Notch-Dll1 pairs. They also confirmed that inhibiting endocytosis reduced the forces exerted on the tethered beads (note that similar forces applied by the simultaneous endocytosis of Notch in receptor-presenting cells could add to the overall force experienced by receptor-ligand pairs). Membrane rigidity in Notch-expressing cells could also modulate the level of force in the system, with cells with pliable membranes expected to experience less pulling force than cells with rigid membranes.

A prevailing hypothesis is that efficient endocytosis (and thereby force generation) is enabled by the ubiquitylation of the intracellular domain (ICD) of Notch ligands by Mind bomb (or Neuralized in flies). While it is still unclear why DSL ligands excel in activation after ICD ubiquitylation, it is clear that ubiquitination by Mib and Neur remains an important regulatory step controlling Notch ligand activity. A recent study from the Blacklow lab provided structural insights into how Mind bomb1 (Mib1) binds the ICDs of ligands to promote their monoubiquitination by solving the X-ray structure of mammalian Mib1 alone and in complex with peptides corresponding to Jag1 and Delta (Guo et al., 2016; McMillan et al., 2015). At its N terminus Mib1 consists of five elements: two Mib-Herc2 domains separated by ZZ zinc-finger domain (forming the MZM), followed by tandem Mib-repeat domains (REP) (Figure 1). C-terminal to MZM-REP are an ankyrin repeat domain of unknown function and three C-terminal ring domains that recruit the E2 ubiquitin-conjugating enzyme. Unexpectedly, the 3D structure of both the Mib-Herc2 and Mib-repeat domains of Mib1 is similar to an SH3 domain despite lack of sequence conservation. Through its N-terminal region, Mib1 binds two short, well-conserved and discontinuous regions on the intracellular tails of DSL ligands: a membrane proximal N-box sequence and a less-conserved C-box sequence separated by approximately 70 residues (Figure 1). MZM-REP crystals soaked with peptides that correspond to the N-box

sequence of Jag1 and Delta show that the N-box binds a highly conserved surface patch on the first Mib-Herc2 domain of Mib1. The authors were unable to determine the X-ray structure of MZM-REP bound to peptides corresponding to the C-box. However, using a combination of structural inferences and biochemical/biophysical binding studies, they showed that the Mib-repeat domains are involved in binding the C-box region of DSL ligands. Notably, cell-based assays show reduced but significantly higher-than-background activation by a Dll1 ligand lacking its ICD (see, for example, Gordon et al., 2015). Moreover, it has been shown that synthetic Notch receptors in which the ECD was replaced by monoclonal antibodies can be activated by ligands without an intracellular tail, and thus without ubiquitylation (Morsut et al., 2016). Why, then, is ubiquitylation required? And how does it mechanistically contribute to endocytosis?

While endocytosis is the best candidate for the pulling-force generator, other force-generating mechanisms have been proposed. Recent evidence suggests that Notch signals can be transduced through filopodial contacts (Cohen et al., 2010; Hunter et al., 2016). Since endocytosis does not occur in filopodia, a potential pulling-force generator could be the active transport mediated by molecular motors (Kerber and Cheney, 2011). Other alternative candidates for producing a pulling force are cell migration and shear stress generated by blood flow (Theodoris et al., 2015), although there is no detailed study on the forces exerted by such mechanisms. Nevertheless, multiple force-generating mechanisms in addition to endocytosis are likely to be capable of activating Notch signaling in vivo.

Spatial Organization and Cell Morphology Dependence in Notch Signaling

An emerging topic in recent years in the Notch field has been the spatial organization of Notch receptors and ligands and the effect of cell and tissue morphology on signaling. This effort has been focused at two levels: the spatial organization of Notch receptors and ligands at the subcellular level, and the effect of cellular and tissue morphology on Notch signaling and Notch-mediated patterning.

Work from the Schweisguth lab provided insight into the complex regulation of Notch receptor distribution during the asymmetric cell division of the sensory organ precursor (SOP) in *Drosophila* (Couturier et al., 2012, 2013). Using live tissue imaging of endogenously tagged Notch-GFP, Couturier et al. showed that, during SOP cytokinesis, Notch is localized at the apical interface between the two daughter cells (pIIa and pIIb), restricting Notch signaling to operate exclusively between these two cells. Furthermore, they showed that the Notch inhibitor Numb, in complex with Sanpodo, regulates the asymmetric distribution of Notch at the cell junction required for the specification of the pIIa and pIIb fates. In their more recent paper (Couturier et al., 2013), the authors further show how directional recycling of Sanpodo-containing endosomes regulates this asymmetric distribution of Notch. These findings highlight the important role of regulation of the membrane distribution of Notch receptors and ligands.

Another nice example for the effect of local distribution of Notch receptors and ligands on asymmetric cell division was recently described by Akanuma et al. (2016). In this work the authors show that the asymmetric division of the V2 neural progenitor cells in the developing zebrafish nervous system is affected by variations in cell shape. They suggest that the DeltaC ligand is asymmetrically enriched to the more elongated side of the V2 cell, creating a bias in ligand concentration that is maintained during mitosis. This bias in local DeltaC concentration is translated to a bias in Notch signaling that is sufficient to define distinct cell fates for the two daughter cells.

In addition to localization of Notch receptors/ligands, the morphological properties of contact area between cells may also contribute to Notch signal strength. While Notch receptors and ligands are often described in the context of apical junctions in epithelial layers (as in the SOP case described above), there are multiple examples for other junction morphologies, including in sprouting angiogenesis (Jakobsson et al., 2010), the germline stem cell niche in *C. elegans* (Byrd et al., 2014; Lee et al., 2016), and the immune synapse (Luty et al., 2007). Recent years have seen a growing interest in the role of cellular protrusions such as filopodia or cytonemes in various developmental processes (Kornberg and Roy, 2014). Several authors have suggested that Notch signals can be mediated by such filopodia in various contexts. Studies from the Baum lab proposed that Notch signaling through dynamic basal protrusions is important in SOP patterning in *Drosophila* (Cohen et al., 2010). It was also suggested that signaling through filopodia allows for an extended range by which prospective SOPs can inhibit neighboring cells, thus allowing for larger spacing between SOP cells. More recent work by Hunter et al. (2016) suggests that differences in the level of signaling between SOP and its direct (cells that share apical contact) and indirect neighbors (cells in contact through filopodia) are important for ordered and timely progression of SOP patterning. However, a recent paper by Troost et al. (2015) provides evidence against the filopodial model of SOP patterning, showing that only cells adjacent to the SOP receive inhibitory Notch signals. Hence, more direct evidence is needed to resolve this controversy.

Two recent studies on pigment patterns in zebrafish provided evidence that Notch signaling can also be transduced through cellular protrusions in vertebrates. Hamada et al. (2014) showed that Notch signaling provides the long-range survival signal from xanthophores (bright pigment cells) to melanophores (dark pigment cells) in adult skin patterns. They suggest that these signals are mediated by long protrusions extended from the melanophores to the xanthophores. Interestingly, they proposed that Notch signaling through protrusions in this system can serve as a long-range signal for a Turing-like patterning process that underlies the formation of stripes. More recently, Eom et al. (2015) used time-lapse microscopy in zebrafish to show that fast-moving projections, termed airinemes, are extended from melanophores. These airinemes, which contain both actin microfilaments and microtubules, carry the Notch ligand Delta and are stabilized upon interaction with xanthophores. Interestingly, no airinemes were observed in melanophores of *Danio albolineatus*, which lack striped patterns. We note, however, that there is still no direct evidence for Notch signaling through filopodia, nor a potential mechanism for how Notch can be activated by ligand-bearing filopodia (see discussion in section on Notch mechanotransduction).

The question of how different contact geometries affect Notch signaling and Notch-mediated patterning was recently treated both theoretically and experimentally in two studies by Khait

et al. (2016) and Shaya et al. (2017). In the first study, Khait et al. analyzed the interplay between membrane dynamics and contact geometry. Two possible scenarios were identified: for relatively large contact areas and/or slow diffusion (e.g., in epithelial contacts), signaling strength is expected to be proportional to the contact area. By contrast, for relatively small contact areas and/or a fast diffusion regime (e.g., filopodia) signaling strength should be independent of contact area but dependent on the diffusion length scale of Notch receptors and ligands. Based on FRAP-TIRF measurements of Dll1 diffusion and endocytosis rates, the authors showed that the transition between the two regimes is expected to occur for contact diameters on the order of 1–2 μm. To experimentally test this prediction, Shaya et al. (2017) directly measured the dependence of Notch signaling on contact area using a bowtie-shaped micro-patterned device with a single sender cell expressing Dll1 ligands and a single receiver cell expressing N1 receptors. Consistent with previous studies (Khait et al., 2016), it was found that Notch signaling was proportional to the contact width, for contact widths ranging from 1 to 40 μm.

But what is the developmental impact of the dependence of Notch signaling on contact? Interestingly, modeling lateral inhibition while taking into account the dependence of signaling on contact area predicts that smaller cells are more likely to become signal-producing cells. Consistent with this prediction, ligand-producing hair cell precursors in the chick inner ear were found to be smaller than their neighbors (Shaya et al., 2017). Thus, cell morphology can influence the outcome of cell fate determination processes.

Proteolytic Cleavage and Charge Distribution at/below the Membrane

The above structural and biophysical studies have revealed significant new insights into the mechanisms of ligand-receptor interaction and force generation. Force generation is required for Notch receptor proteolysis with the γ-secretase enzyme ultimately freeing the NICD polypeptide from the membrane and into the cytoplasm. In a tour de force effort using single-particle cryo-EM methods, the Yigong Shi and Sjors Scheres laboratories determined the structure of the human γ-secretase to 3.4 Å resolution (Bai et al., 2015a, 2015b; Lu et al., 2014; Sun et al., 2015). γ-Secretase is a 170 kDa integral membrane protein complex required for the intramembrane S3 cleavage of many type I proteins, including Notch and the amyloid precursor protein. It is composed of four proteins, contributing 20 transmembrane (TM) spanning helices. Either Presenilin1 or Presenilin2 provides the catalytic domain. Pen-2 is required for maturation of Presenilin; Aph-1a (or Aph-1b) is required for proper assembly of the γ-secretase complex. Finally, Nicastrin, which is not needed for catalytic activity or substrate recognition (Zhao et al., 2010) is involved in complex stabilization and perhaps substrate selection (Li et al., 2014a). The cryo-EM data showed that the 20 TM helices adopt a horseshoe-like structure with a Presenilin and an Aph-1 molecule located in the center and the ECD of Nicastrin forming a head domain that sits atop the hollow region of the horseshoe (Figure 1). Aph-1 appears to function as a scaffold, supporting the single Nicastrin TM helix and the flexible structure of Presenilin. Notably, distinct γ-secretase complexes are present in different cell types. Loss of Psen2/Aph1b complexes is tolerated, presumably due to a lesser role in Notch biology (Serneels et al., 2005). However, they may have unique disease-modulating activity in specific subcellular compartments (Sannerud et al., 2016). Interestingly, the aspartate residues required for intramembrane catalysis are located on the convex side of the TM horseshoe, i.e., distal from the putative substrate binding region, and are ~10 Å apart, too far for catalysis. These findings suggest that a substantial conformational change must occur in γ-secretase following substrate binding, possibly involving the two lobes of Nicastrin, in order to bring the catalytic aspartates into alignment for proteolysis. In addition, the Shi lab determined the γ-secretase structure bound to the inhibitor DAPT (N-[N-(3,5-difluorophenacetyl)-L-alanyl]-S-phenylglycine t-butyl ester; Bai et al., 2015a). DAPT binds in a hydrophobic pocket near the Presenilin active site, which results in a pronounced rigidification of the Presenilin TM segments, but little to no structural changes in Aph-1, Nicastrin, and Pen-2. This inhibitor may act by reducing the likelihood of conformational changes needed for catalysis. Another peptidomimetic inhibitor, compound E (S,S)-2-[2-(3,5-difluorophenyl)-acetylamino]-N-(1-methyl-2-oxo-5-phenyl-2,3-dihydro-1H-benzo[e][1,4]diazepin-3-yl)-propionamide), binds to the PS1 N terminus and induces a conformational change that reduces substrate binding at the substrate-docking site (Li et al., 2014b). Interestingly, the authors identified a reciprocal allosteric interaction between the docking site and the compound E binding site: a bound substrate paradoxically increased compound E binding, and thus inhibition. The authors speculated that these reciprocal interactions reveal the gating mechanism that underlies access of substrate to the catalytic site.

Free at Last: The Latest Insights on NICD Function in the Nucleus

Once Notch is cleaved by γ-secretase, NICD peptides are released from the membrane. However, γ-secretase generates several NICD molecules with different compositions at their amino termini. Molecules with an N-terminal Val or Met are long lived, but other amino acids may be tolerated in a cell-type-specific manner. Immediately below the new amino terminus lies the high-affinity Notch/RBPJ interaction domain containing the WFP tripeptide. Structural studies reveal that a relatively short N-terminal region around the WFP becomes ordered when bound to CSL (Choi et al., 2012; Friedmann et al., 2008), but the molecular properties of the entire RBPJ associated molecule (RAM) linker region have been poorly defined. Between the WFP region and the low-affinity ANK domain lies the RAM domain; ongoing biophysical studies in the Barrick lab have continued to provide insights into its structure and function. NMR and analytical ultracentrifugation studies of RAM by Bertagna et al. (2008) and Sherry et al. (2015) have shown that the RAM forms a compact intrinsically disordered protein that is stabilized by electrostatic interactions. Using a series of insertion and deletion mutations within this region, the authors went on to show that its length has been tuned to optimize formation of the activation complex; shorter and longer versions of RAM/ANK linker are deficient in reporter activation assays. However, Sherry and colleagues also identified several regions within the RAM/ANK linker that have stronger effects on activation than would be predicted from polymer statistics. This finding suggests that deletion of these regions has sequence-specific effects on the interactions between CSL and NICD, likely changing the compaction of

RAM and thereby indirectly affecting formation of the CSL-NICD-mastermind (MAM) activation complex.

How Is Information Encoded in CSL Binding Sites within a cis-Regulatory Module to Yield Cell/Target Gene Specificity?

Notch, β-catenin, and Yap/Taz are transcription factors in the sense that they regulate transcription, but none directly binds DNA. Instead, all three seek DNA binding partners, and only NICD associates with a single transcription factor, CSL (RBPJ in vertebrate species). Studies across organisms revealed that all cell types use this common core complex (CSL/NICD) to mediate Notch transcriptional responses, and yet they often do so in a largely cell-specific manner. How the same Notch signal can regulate distinct sets of target genes within different cell types has been a major area of study over the past two decades. Although the events surrounding Notch target selection are still shrouded in mystery, two main themes have emerged: (1) CSL transcription factor binding site architecture, affinity, and combinatorial *cis*-regulatory logic differ between enhancers and are likely to contribute to target gene specificity, and (2) CSL and CSL/NICD can recruit a large number of additional chromatin and transcriptional regulatory proteins to both positively and negatively affect gene expression. Here, we review the contribution of each in generating Notch transcriptional responses.

Studies focused on defining how CSL DNA binding sites contribute to transcription outputs have begun to shed light on how orientation, spacing, affinity, and integration with additional inputs by *cis*-regulatory modules (CRMs) shape Notch-dependent contributions (Figure 2). Perhaps the best studied of these parameters has been the Su(H)-paired-sites (SPS, or Su(H)-paired-sites) that were originally described in the enhancer of split E(spl) complex in *Drosophila*, and have been found in CRMs of genes from insects to mammals (Bailey and Posakony, 1995; Hass et al., 2015; Liu and Posakony, 2012, 2014; Nellesen et al., 1999). SPS sites consist of two CSL sites that are found in a specific orientation (head-to-head) and spacing (~15–17 nucleotides apart). Biochemical and structural studies revealed that SPS sites can form cooperative complexes by recruiting CSL/MAML/NICD to each CSL site with dimerization contacts mediated by adjacent NICD molecules (Arnett et al., 2010). Interestingly, no such cooperative interactions have been described for CSL/co-repressor complexes on SPS sites, suggesting that target CRMs containing this CSL DNA binding site configuration will likely behave differently than targets containing non-cooperative CSL binding sites.

While originally described in the commonly regulated E(spl) and Hes target genes, recent findings have described the presence of SPS sites within a variety of Notch targets. For example, the mouse *Myc* (Herranz et al., 2014; Yashiro-Ohtani et al., 2014) and *Nrarp* (Hass et al., 2015; Wang et al., 2014) genes are regulated by SPS-containing super-enhancers. Hass et al. used a DNA adenine methyltransferase (DAM) protein-complementation assay (called split-DamID or SpDamID) to identify many potential dimer-dependent Notch targets. In this assay, the DAM enzyme is split into two parts (D and AM) and fused to different proteins binding within a complex (or in proximity to each other), enabling reconstitution of an active DNA adenine methyltransferase and labeling of the DNA strand to which they bind (Hass et al., 2015). By fusing the D and AM components to separate Notch wild-type or dimerization-deficient alleles, only genomic regions that co-recruit at least two nearby CSL/MAM/NICD complexes will complement DAM and methylate DNA. This assay could distinguish between dimer-dependent SPS sites (which were not labeled by the $NICD^{R1947A/R1954A}$ dimerization-deficient pair, but are labeled by all other Notch-containing pairs) versus two adjacent dimer-independent CSL sites (that were labeled by all complexes including $NICD^{R1947A}$ monomers), enabling the authors to use bioinformatic and reporter assays to confirm the presence of two distinct SPS sites within the *Nrarp* Notch target gene. Interestingly, and perhaps reflecting a general rule, both *Nrarp* SPS sites contain only one high-affinity CSL site and one low-affinity (also called cryptic) CSL site in the preferred spacing/orientation. Genome-wide analysis of enriched SPS within the NICD/NICD SpDamID-labeled fragments that were not labeled by dimer-deficient $NICD^{R1947A}$ molecules indicate that many CRMs are likely to contain Notch dimer-dependent SPS sites.

In addition to CSL binding site configuration, there is emerging evidence that low-affinity CSL binding sites may be critical for regulating cell-specific outputs (Ramos and Barolo, 2013; Swanson et al., 2010, 2011). For example, recent data on a Notch target gene in the *Drosophila* eye demonstrates that CSL binding affinity can affect cell-specific transcription downstream of Notch. The *sparkling* (*spa*) enhancer, which regulates the expression of the *Drosophila* Pax2 gene in cone cells of the eye, contains five CSL sites (none with the SPS orientation/spacing) that contribute to Notch-dependent transcription. However, none of the *spa* CSL sites matches the consensus-binding site, suggesting they are all low-affinity sites. When Swanson et al. changed the CSL sites within *spa* to the consensus sequence, not only was the enhancer activated to higher levels in cone cells, it was now expressed within additional Notch-dependent cell types (photoreceptors) within the eye. Hence, at least in this case, cell-type specific activation via Notch signaling required low-affinity CSL sites.

Not surprisingly, endogenous Notch-dependent gene expression requires CRMs that contain additional transcription factor binding sites. Perhaps the best known combinatorial code that has been established for Notch targets is the SPS plus proneural factor binding sites (called either E-box sites or P sites) found in several E(spl) and Hes targets (Castro et al., 2005; Cave and Caudy, 2008; Cave et al., 2005, 2011). Proneural factors are basic-helix-loop-helix (bHLH) proteins that form homo- or heterodimers (typically with the ubiquitous E12/E47 proteins) on CANNTG E-box sequences to activate gene expression and promote neurogenesis. Studies from the Posakony and Caudy labs have shown that nearby SPS + E/P sites cooperate to yield strong activation of E(spl)/Hes factors during lateral inhibition in the nervous system. While the exact mechanism of integration between proneural and CSL complexes is unclear, there is some evidence that the N terminus of the *Drosophila* E-protein (daughterless) can physically interact with Su(H) to stimulate transcription on SPS-dependent reporters. This finding suggests a model where nearby SPS and E/P sites recruit transcription complexes that interact to synergize gene expression. However, it currently remains unclear what the constraints (spacing, orientation, etc.) are for the SPS + E/P sites to mediate this synergy. It also remains unclear if this requirement is conserved in vertebrates.

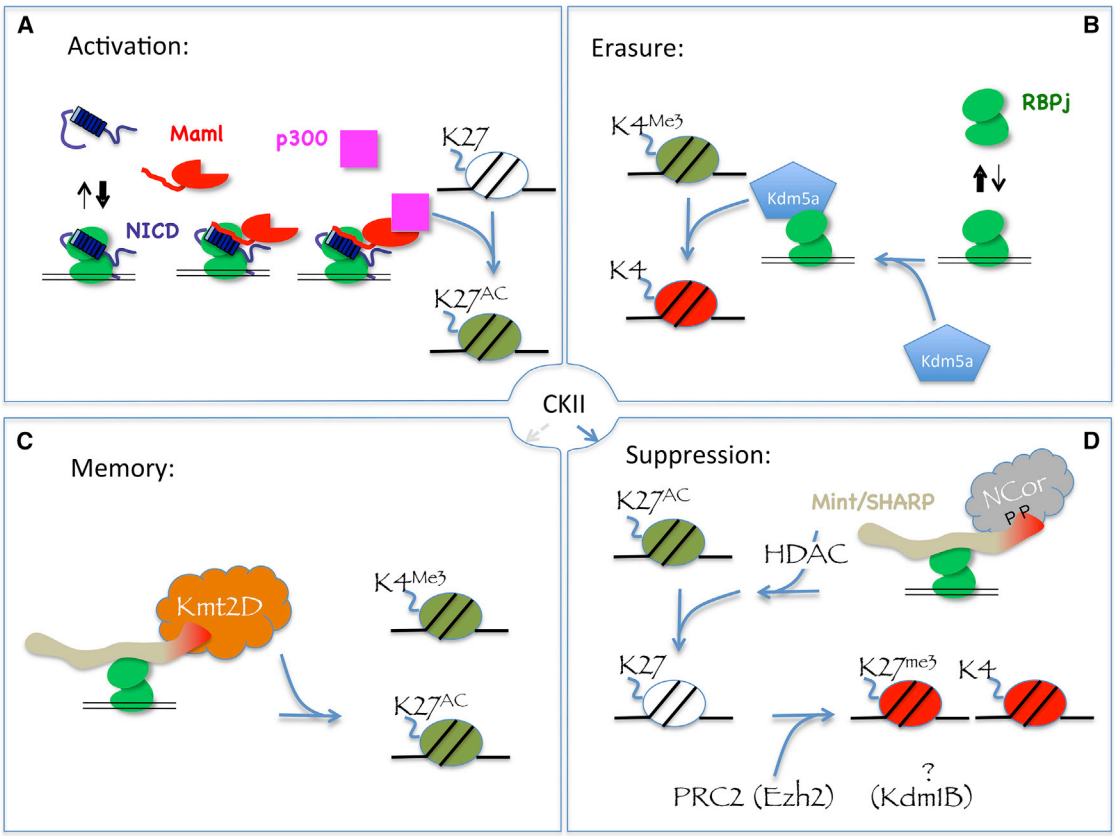

Figure 2. Regulating Transcription

(A) CSL (green) interacts with NICD (dark blue) through the high-affinity WFP tripeptide (hidden by RBPJ) and the low-affinity ANK domain, positioned at optimal distance by the RAM domain. MAML1 (red) binds to the interface between the ANK and the CSL, and recruits the histone acetylases p300 (pink). P300 convers H3K27 to H3K27ac, a modification enriched in enhancers. Details on specifically how the Notch TAD stimulates transcription are lacking.

(B) In the absence of NICD, the short-term consequences includes recruitment of Kdm5a to the chromatin and loss of H3K4me3. This is a reversible state.

(C) If CKII activity is low or absent, Mint/SHARP will instead recruit Kmt2D which will maintain chromatin in the permissive H3K27ac and H3K4me3 state, bookmarking the site for future Notch-mediated activation.

(D) In cells lacking NICD and containing active CKII, RBPJ recruits phosphorylated Mint/SHARP, which binds to NCor. This complex is associated with histone deacetylases (HDAC) that restore H3K27. The Ezh2 protein in the PRC2 complex than converts H3K27 to H3K27me3, establishing a repressed state propagated further by removal of methyl groups from K4 by Kdm1b.

Other transcriptional inputs have also been found in association with CSL binding sites (Liu and Posakony, 2012, 2014). For example, Runx binding sites were found to be associated with potential CSL-regulated enhancers in a number of studies in both *Drosophila* and vertebrates. Using the SpDamID method, Hass et al. (2015) found that many genomic regions bound by NICD were highly enriched for nearby Runx binding sites. Thus, these data support the idea that CRMs commonly integrate both Runx and CSL inputs to regulate target gene expression downstream of Notch signals.

A well-studied example of Notch and Runx integration is the regulation of the *Bcl11b* gene in T cells (Kueh et al., 2016; Li et al., 2013; Rothenberg, 2012). *Bcl11b* transcription is regulated by multiple transcription factors including Gata3, TCF1, Runx1, and CSL/NICD. Aside from the fact that *Gata3* and *TCF7* (the gene coding for Tcf1) are Notch targets, analysis of *Bcl11b* regulation demonstrated a clear role for NICD as a frequency modulator, the very function assigned to enhancer elements (Kueh et al., 2016). To understand how *Bcl11b* is regulated in single cells undergoing β selection, the investigators inserted a florescent protein downstream of the *Bcl11b* transcript. Having demonstrated the fidelity of their reporter, they noted three phases in *Bcl11b* regulation: an early, pre-lineage commitment phase, which required TCF1 and Gata3 (and thus indirectly required Notch signals). This step prepared the locus for a second phase that regulated the timing and frequency of *Bcl11b* expression and was dependent on NICD binding. Importantly, whereas both the activation and maintenance of a distant enhancer in cMyc in T cells depended on the presence and concentration of NICD (Herranz et al., 2014; Yashiro-Ohtani et al., 2014), *Bcl11b* maintenance was independent of NICD concentration and instead required Runx1, which regulated the amplitude of *Bcl11b* expression. Coupled with the ability of the Notch complex to recruit the histone acetylase p300, chromatin modification in the vicinity of the enhancer or, following looping in the vicinity of the promoter, could contribute to this mechanism (Figure 2A).

However, it is less clear if the combination of Runx and CSL binding sites is sufficient to yield specific outputs. In fact, the thorough dissection of the *spa* enhancer in *Drosophila* suggests that relatively simple combinatorial codes fail to adequately

explain cell-specific responses to Notch signals. The early studies by Banerjee and others suggested that the *spa* enhancer integrates three different transcription inputs to yield cone-cell-specific gene expression: the five low-affinity CSL sites mentioned above, lozenge (a Runx homolog) binding sites, and binding sites for the ETS transcription factors that are regulated by receptor tyrosine kinase signaling (Flores et al., 2000). Interestingly, cross-species studies revealed that the *spa* enhancer from other *Drosophila* species evolved quickly and yet still maintained cone-cell-specific expression when tested in *Melanogaster*. Sequence analysis revealed that, while each of these regulatory elements had relatively few blocks of sequence conservation, they did all have CSL + Lz + ETS sites, suggesting that this simple code could explain cone-cell-specific gene expression (Swanson et al., 2010, 2011). Although Runx and ETS sites are also co-enriched with RBPJ sites in vertebrate enhancers (Hass et al., 2015; Wang et al., 2011, 2014), synthetic attempts to engineer enhancers containing CSL + Lz + ETS sites failed to yield accurate gene expression patterns. Moreover, Swanson et al. performed a thorough dissection of the *Melanogaster spa* enhancer and found that changes in spacing between sites can result in ectopic expression in inappropriate cell types and that additional TF binding sites contribute to cell-specific gene expression. Thus, while the combinatorial codes that are being uncovered have revealed conserved cooperating factors required for proper Notch-regulated activity, we still do not have a sufficient functional understanding of their integration to enable us to engineer and/or predict the behaviors of these elements in vivo.

Lastly, while the majority of the studies above have focused on the characterization of individual CRMs, genomic studies have also begun to significantly impact our understanding of Notch target selection and regulation. For example, while the affinity of CSL to DNA is relatively modest (~60–1,000 nM; Friedmann and Kovall, 2010; Torella et al., 2014) and does not change in affinity or specificity when in complex with NICD in vitro (Del Bianco et al., 2010; Friedmann et al., 2008), the in vivo NICD/CSL complex appears to bind better to DNA than CSL alone. Indeed, genome-wide analyses identified enrichment of CSL at enhancers in both *Drosophila* (Skalska et al., 2015) and T cells (Wang et al., 2014) after a short pulse of Notch stimulation. How NICD stimulates CSL DNA binding is currently unclear but it could be through either enhanced dwell times on enhancers and/or via chromatin acetylation (see below) and the opening of additional DNA binding sites within the CRM. However, we should also note that, although NICD/CSL binds primarily to enhancers, only a small fraction of all possible binding sites located within available enhancers and open chromatin regions are bound by this complex in flies (Skalska et al., 2015) or mammalian cells (Hass et al., 2015; Wang et al., 2014). Hence, it still remains largely unclear how CSL/NICD complexes select the appropriate combinations of target genes within the genome.

NICD Maintains Gene Expression by Modulating the Interactions with Chromatin and/or Modifiers

The above section deals largely with how the CSL/NICD complex finds the appropriate target genes within the genome. Another intriguing question is: once bound, how does the CSL/NICD complex mediate an appropriate output? The large-scale purification of NICD1 from human T-All cells (Yatim et al., 2012) identified multiple chromatin modifiers as additional potential partners, including the remodeling factor PBAF subunits BRG1 and PB1, the histone demethylase LSD1 (Curtis et al., 2011; Di Stefano et al., 2011; Mulligan et al., 2011), members of the Cohesin complex (*Mah2,Pdd5A, Smc3,*and *Smc1A*), the SWI/SNF complex (*Hltf,Snf2H*), four members of the repressive NuRD complex (*Hdac1, Chd4, Gatad2B*, and *Rbbp4*) and two members of PRC1 (*Ring1* and *Rnf2*). Interactions with repressive complexes may help recruit NICD/CSL to closed chromatin where CSL alone could not bind. Alternatively, these factors are recruited to promoters that NICD helps repress.

In vertebrates, *Bcl11b* represents a locus that no longer depends on active Notch signaling after expression is induced. However, many T cell genes require NICD for their maintenance, including *Deltex, Hes1, CD25*, and *PreT* (Liefke et al., 2010). What happens to such NICD-regulated sites after NICD turnover? Interestingly, transient inhibition of γ-secretase in a pre-T cell line resulted in loss of trimethylation of lysine-4 on histone-3 (H3K4me3) in the vicinity of CSL binding sites, while retaining these marks over the gene body. Methyl groups had a half-life of about 5 hr (Liefke et al., 2010), corresponding to ~3 half-lives for the NICD protein. Investigating this phenomenon, Oswald, Borggrefe, and their colleagues noted that once NICD was degraded, RBPJ recruited the demethylase Kdm5a that led to disappearance of active H3K4me3 near the transcription start site (Figure 2B). Washing the inhibitor away within 24 hr permitted reactivation of target genes with corresponding re-methylation and accumulation of H3K4me3. This interaction is conserved across species as the reduction in the Kdm5a homolog Lid resulted in enhancement of Notch gain-of-function in *Drosophila* (Liefke et al., 2010). Prolonged absence of NICD was expected to allow recruitment of the adaptor Mint/SHARP/SPEN. This large adaptor protein interacts with several transcription factors, including Msx2 and RBPJ, to bridge between RBPJ and repressor proteins such as NCor/SMRT (Tsuji et al., 2007; Yabe et al., 2007).

A recent study explored the Mint/SHARP/SPEN repression complex in some detail and reported a surprising observation (Figures 2C and 2D) (Oswald et al., 2016). The C-terminal SPOC domain of the Mint/SHARP/SPEN protein bound to the MLL4 activator complex via Kmt2D, a H3K4 methyltransferase that generates H3K4me3 marks. The investigators found that NCor does not bind to Mint/SHARP/SPEN unless it is phosphorylated by CKII on a conserved LSDSD motif; once phosphorylated, NCor effectively compete with Kmt2D for Mint/SHARP/SPEN binding. The recruitment of NCor represses transcription, whereas the recruitment of the MLL4 complex to RBPJ-bound regions enhances the retention of transcription-ready chromatin (Oswald et al., 2016), reminiscent of reports that Mint enhanced transcription mediated by Runx2 (Sierra et al., 2004).

These remarkable observations offer the following interpretation. On certain loci, a pulse of Notch activation releases NICD, which increases the likelihood of transcription by a yet-to-be-described mechanism. Once NICD degrades, several scenarios may unfold consistent with selection of different, context-specific outcomes. First, factors like Runx1 could maintain expression (as with *Bcl11b* in T cells where Notch contributes to linage commitment). Second, Kdm5A recruitment by RBPJ will remove the methyl groups from H3K4 at specific sites. What follows will

depend on the level of CKII activity. When CKII activity is low, Mint/SHARP/SPEN will bridge Kmt2D with RBPJ, ensuring the maintenance of H3K4me3 marks and maintaining the locus in a transcription-ready state for the next round of Notch activation (Figure 2C). By contrast, when CKII activity is high, Mint/SHARP/SPEN will bridge NCor and its associated HDAC to RBPJ, removing acetyl groups from $H3K27^{AC}$ at enhancers bound by the RBPJ/NICD/MAML/p300 complexes (Figure 2D). The Ezh2 enzyme in the PRC2 complex may then methylate H3K27me3 to establish a repressed state. In parallel, demethylation of H3K4me3 will continue to spread, mediated by another PRC2 complex protein, Kdm1B. One can imagine that following a division, one daughter could be in a $CK2^{LO}$ regime and the other in a $CK2^{HI}$ regime (perhaps exposed to a higher Wnt signal), altering the epigenetic landscape of genes amenable to Notch regulation and ensuring selection of different fates by daughter cells.

It is well established that CSL is needed to activate transcription from all Notch target genes, but its role as a repressor is less well defined. Moreover, the corepressors that bind CSL to mediate repression, such as Hairless in *Drosophila*, and Mint/SHARP/SPEN and KyoT2 (also known as Fhl1) in mammals, appear to be divergent in different species. The Kovall lab has used a combination of structural, biophysical, and biochemical/cellular techniques to deepen our understanding of how corepressors interact with CSL to prevent transcription at Notch target genes (Collins et al., 2014; Yuan et al., 2016). KyoT2 was identified in a yeast two-hybrid screen looking for RBPJ binding partners. It is a multi-domain corepressor protein that contains N-terminal LIM domains followed by a region that bears sequence similarity to the RAM domain of Notch. This RAM-like sequence of KyoT2 binds the BTD of RBPJ with approximately 10 nM affinity (Collins et al., 2014). The RBPJ-KyoT2 X-ray structure reveals that KyoT2 binds the BTD of CSL in a similar fashion as RAM, suggesting that in the nucleus KyoT2 is tethered to RBPJ via its high-affinity interaction to the BTD (Collins et al., 2014). This likely serves to localize the LIM domains at Notch target genes, which have been shown to interact with components of the Polycomb repression complex.

Hairless is the major antagonist of Notch signaling in *Drosophila*. Hairless directly binds the fly CSL ortholog Su(H) with high affinity and also interacts with the corepressors Groucho and CtBP. Recently, Yuan et al. (2016) determined the X-ray structure of Su(H)-Hairless bound to DNA. As predicted from earlier studies, Hairless binds the CTD of Su(H) (Maier et al., 2011). Surprisingly, Hairless binding induces a substantial conformational change in CTD, which would preclude binding by NICD or Mastermind. Despite their partially overlapping binding sites, based on the complex structure, the authors were able to design mutations that affect Hairless binding, but leave interactions with NICD and Mastermind largely unperturbed. These mutants were characterized in *Drosophila* S2 cells and in vivo assays in the fly, laying the groundwork for designing and analyzing flies that are selectively defective in repression or activation, but not both activities.

Unanswered Questions

Despite the progress, much remains to be learned about the Notch signaling pathway. In addition to questions posed within this review, many others remain. For example, can different ligands result in the selection of different targets, and, if so, by what mechanism? Are all Notch targets activated stochastically (Lee et al., 2016) or are common targets such as E(spl)/Hes bound preferentially? Why are some tissues/targets dose sensitive but most are not? What is the role of SPS/dimerization in Notch biology? What is the mechanism enabling force generation at an extended filopodia, and what role do they play in vertebrate biology? How can NICD change the occupancy of CSL on its targets? What specific function is performed by NICD, and how does it fit in the transcriptional "logic" of a given CRM? And, most pressing for the general public, how can one safely and specifically modulate Notch signaling to produce a desired therapeutic effect with minimal untoward effects? How does ADAM10 recognize and engage the unmasked S2 processing site in response to force? And how does ADAM10 recognition in physiologic contexts differ from pathologic recognition by ADAM17? The answers are within reach, but not without continued investment in time and resources.

REFERENCES

Akanuma, T., Chen, C., Sato, T., Merks, R.M., and Sato, T.N. (2016). Memory of cell shape biases stochastic fate decision-making despite mitotic rounding. Nat. Commun. *7*, 11963.

Andrawes, M.B., Xu, X., Liu, H., Ficarro, S.B., Marto, J.A., Aster, J.C., and Blacklow, S.C. (2013). Intrinsic selectivity of notch 1 for delta-like 4 over delta-like 1. J. Biol. Chem. *288*, 25477–25489.

Arnett, K.L., Hass, M., McArthur, D.G., Ilagan, M.X., Aster, J.C., Kopan, R., and Blacklow, S.C. (2010). Structural and mechanistic insights into cooperative assembly of dimeric Notch transcription complexes. Nat. Struct. Mol. Biol. *17*, 1312–1317.

Aster, J.C., Pear, W.S., and Blacklow, S.C. (2017). The varied roles of notch in cancer. Annu. Rev. Pathol. *12*, 245–275.

Bai, X.C., Rajendra, E., Yang, G., Shi, Y., and Scheres, S.H. (2015a). Sampling the conformational space of the catalytic subunit of human gamma-secretase. eLife *4*, e11182.

Bai, X.C., Yan, C., Yang, G., Lu, P., Ma, D., Sun, L., Zhou, R., Scheres, S.H., and Shi, Y. (2015b). An atomic structure of human gamma-secretase. Nature *525*, 212–217.

Bailey, A.M., and Posakony, J.W. (1995). Suppressor of Hairless directly activates transcription of enhancer of split complex genes in response to Notch receptor activity. Genes Dev. *9*, 2609–2622.

Benedito, R., Roca, C., Sorensen, I., Adams, S., Gossler, A., Fruttiger, M., and Adams, R.H. (2009). The notch ligands Dll4 and Jagged1 have opposing effects on angiogenesis. Cell *137*, 1124–1135.

Bertagna, A., Toptygin, D., Brand, L., and Barrick, D. (2008). The effects of conformational heterogeneity on the binding of the Notch intracellular domain to effector proteins: a case of biologically tuned disorder. Biochem. Soc. Trans. *36*, 157–166.

Bray, S.J. (2016). Notch signalling in context. Nat. Rev. Mol. Cell Biol. *17*, 722–735.

Byrd, D.T., Knobel, K., Affeldt, K., Crittenden, S.L., and Kimble, J. (2014). A DTC niche plexus surrounds the germline stem cell pool in *Caenorhabditis elegans*. PLoS One *9*, e88372.

Castro, B., Barolo, S., Bailey, A.M., and Posakony, J.W. (2005). Lateral inhibition in proneural clusters: cis-regulatory logic and default repression by Suppressor of Hairless. Development *132*, 3333–3344.

Cave, J.W., and Caudy, M.A. (2008). Promoter-specific co-activation by Drosophila mastermind. Biochem. Biophys. Res. Commun. *377*, 658–661.

Cave, J.W., Loh, F., Surpris, J.W., Xia, L., and Caudy, M.A. (2005). A DNA transcription code for cell-specific gene activation by notch signaling. Curr. Biol. *15*, 94–104.

Cave, J.W., Xia, L., and Caudy, M. (2011). Differential regulation of transcription through distinct Suppressor of Hairless DNA binding site architectures during Notch signaling in proneural clusters. Mol. Cell. Biol. *31*, 22–29.

Chillakuri, C.R., Sheppard, D., Ilagan, M.X., Holt, L.R., Abbott, F., Liang, S., Kopan, R., Handford, P.A., and Lea, S.M. (2013). Structural analysis uncovers lipid-binding properties of Notch ligands. Cell Rep. *5*, 861–867.

Choi, S.H., Wales, T.E., Nam, Y., O'Donovan, D.J., Sliz, P., Engen, J.R., and Blacklow, S.C. (2012). Conformational locking upon cooperative assembly of notch transcription complexes. Structure *20*, 340–349.

Chowdhury, F., Li, I.T., Ngo, T.T., Leslie, B.J., Kim, B.C., Sokoloski, J.E., Weiland, E., Wang, X., Chemla, Y.R., Lohman, T.M., et al. (2016). Defining single molecular forces required for Notch activation using nano yoyo. Nano Lett. *16*, 3892–3897.

Cohen, M., Georgiou, M., Stevenson, N.L., Miodownik, M., and Baum, B. (2010). Dynamic filopodia transmit intermittent Delta-Notch signaling to drive pattern refinement during lateral inhibition. Dev. Cell *19*, 78–89.

Collins, K.J., Yuan, Z., and Kovall, R.A. (2014). Structure and function of the CSL-KyoT2 corepressor complex: a negative regulator of Notch signaling. Structure *22*, 70–81.

Cordle, J., Johnson, S., Tay, J.Z., Roversi, P., Wilkin, M.B., de Madrid, B.H., Shimizu, H., Jensen, S., Whiteman, P., Jin, B., et al. (2008). A conserved face of the Jagged/Serrate DSL domain is involved in Notch trans-activation and cis-inhibition. Nat. Struct. Mol. Biol. *15*, 849–857.

Couturier, L., Vodovar, N., and Schweisguth, F. (2012). Endocytosis by Numb breaks Notch symmetry at cytokinesis. Nat. Cell Biol. *14*, 131–139.

Couturier, L., Mazouni, K., and Schweisguth, F. (2013). Numb localizes at endosomes and controls the endosomal sorting of notch after asymmetric division in Drosophila. Curr. Biol. *23*, 588–593.

Curtis, B.J., Zraly, C.B., Marenda, D.R., and Dingwall, A.K. (2011). Histone lysine demethylases function as co-repressors of SWI/SNF remodeling activities during Drosophila wing development. Dev. Biol. *350*, 534–547.

D'Souza, B., Meloty-Kapella, L., and Weinmaster, G. (2010). Canonical and non-canonical notch ligands. Curr. Top. Dev. Biol. *92*, 73–129.

Del Bianco, C., Vedenko, A., Choi, S.H., Berger, M.F., Shokri, L., Bulyk, M.L., and Blacklow, S.C. (2010). Notch and MAML-1 complexation do not detectably alter the DNA binding specificity of the transcription factor CSL. PLoS One *5*, e15034.

Di Stefano, L., Walker, J.A., Burgio, G., Corona, D.F., Mulligan, P., Naar, A.M., and Dyson, N.J. (2011). Functional antagonism between histone H3K4 demethylases in vivo. Genes Dev. *25*, 17–28.

Eom, D.S., Bain, E.J., Patterson, L.B., Grout, M.E., and Parichy, D.M. (2015). Long-distance communication by specialized cellular projections during pigment pattern development and evolution. eLife *4*, e12401.

Flores, G.V., Duan, H., Yan, H., Nagaraj, R., Fu, W., Zou, Y., Noll, M., and Banerjee, U. (2000). Combinatorial signaling in the specification of unique cell fates. Cell *103*, 75–85.

Friedmann, D.R., and Kovall, R.A. (2010). Thermodynamic and structural insights into CSL-DNA complexes. Protein Sci. *19*, 34–46.

Friedmann, D.R., Wilson, J.J., and Kovall, R.A. (2008). RAM-induced allostery facilitates assembly of a notch pathway active transcription complex. J. Biol. Chem. *283*, 14781–14791.

Garg, V., Muth, A.N., Ransom, J.F., Schluterman, M.K., Barnes, R., King, I.N., Grossfeld, P.D., and Srivastava, D. (2005). Mutations in NOTCH1 cause aortic valve disease. Nature *21*, 180–184.

Ge, C., and Stanley, P. (2008). The O-fucose glycan in the ligand-binding domain of Notch1 regulates embryogenesis and T cell development. Proc. Natl. Acad. Sci. USA *105*, 1539–1544.

Gordon, W.R., Zimmerman, B., He, L., Miles, L.J., Huang, J., Tiyanont, K., McArthur, D.G., Aster, J.C., Perrimon, N., Loparo, J.J., et al. (2015). Mechanical allostery: evidence for a force requirement in the proteolytic activation of notch. Dev. Cell *33*, 729–736.

Groot, A.J., Cobzaru, C., Weber, S., Saftig, P., Blobel, C.P., Kopan, R., Vooijs, M., and Franzke, C.W. (2013). Epidermal ADAM17 is dispensable for notch activation. J. Invest. Dermatol. *133*, 2286–2288.

Guo, B., McMillan, B.J., and Blacklow, S.C. (2016). Structure and function of the Mind bomb E3 ligase in the context of Notch signal transduction. Curr. Opin. Struct. Biol. *41*, 38–45.

Hamada, H., Watanabe, M., Lau, H.E., Nishida, T., Hasegawa, T., Parichy, D.M., and Kondo, S. (2014). Involvement of Delta/Notch signaling in zebrafish adult pigment stripe patterning. Development *141*, 318–324.

Hambleton, S., Valeyev, N.V., Muranyi, A., Knott, V., Werner, J.M., McMichael, A.J., Handford, P.A., and Downing, A.K. (2004). Structural and functional properties of the human notch-1 ligand binding region. Structure *12*, 2173–2183.

Harvey, B.M., Rana, N.A., Moss, H., Leonardi, J., Jafar-Nejad, H., and Haltiwanger, R.S. (2016). Mapping sites of O-glycosylation and fringe elongation on drosophila notch. J. Biol. Chem. *291*, 16348–16360.

Hass, M.R., Liow, H.H., Chen, X., Sharma, A., Inoue, Y.U., Inoue, T., Reeb, A., Martens, A., Fulbright, M., Raju, S., et al. (2015). SpDamID: marking DNA bound by protein complexes identifies notch-dimer responsive enhancers. Mol. Cell *59*, 685–697.

Herranz, D., Ambesi-Impiombato, A., Palomero, T., Schnell, S.A., Belver, L., Wendorff, A.A., Xu, L., Castillo-Martin, M., Llobet-Navas, D., Cordon-Cardo, C., et al. (2014). A NOTCH1-driven MYC enhancer promotes T cell development, transformation and acute lymphoblastic leukemia. Nat. Med. *20*, 1130–1137.

Hunter, G.L., Hadjivasiliou, Z., Bonin, H., He, L., Perrimon, N., Charras, G., and Baum, B. (2016). Coordinated control of Notch/Delta signalling and cell cycle progression drives lateral inhibition-mediated tissue patterning. Development *143*, 2305–2310.

Jakobsson, L., Franco, C.A., Bentley, K., Collins, R.T., Ponsioen, B., Aspalter, I.M., Rosewell, I., Busse, M., Thurston, G., Medvinsky, A., et al. (2010). Endothelial cells dynamically compete for the tip cell position during angiogenic sprouting. Nat. Cell Biol. *12*, 943–953.

Kakuda, S., and Haltiwanger, R.S. (2017). Deciphering the fringe-mediated notch code: identification of activating and inhibiting sites allowing discrimination between ligands. Dev. Cell *40*, 193–201.

Kerber, M.L., and Cheney, R.E. (2011). Myosin-X: a MyTH-FERM myosin at the tips of filopodia. J. Cell Sci. *124*, 3733–3741.

Kershaw, N.J., Church, N.L., Griffin, M.D., Luo, C.S., Adams, T.E., and Burgess, A.W. (2015). Notch ligand delta-like1: X-ray crystal structure and binding affinity. Biochem. J. *468*, 159–166.

Khait, I., Orsher, Y., Golan, O., Binshtok, U., Gordon-Bar, N., Amir-Zilberstein, L., and Sprinzak, D. (2016). Quantitative analysis of delta-like 1 membrane dynamics elucidates the role of contact geometry on notch signaling. Cell Rep. *14*, 225–233.

Kopan, R., and Ilagan, M.X. (2009). The canonical notch signaling pathway: unfolding the activation mechanism. Cell *137*, 216–233.

Kornberg, T.B., and Roy, S. (2014). Cytonemes as specialized signaling filopodia. Development *141*, 729–736.

Kueh, H.Y., Yui, M.A., Ng, K.K., Pease, S.S., Zhang, J.A., Damle, S.S., Freedman, G., Siu, S., Bernstein, I.D., Elowitz, M.B., et al. (2016). Asynchronous combinatorial action of four regulatory factors activates Bcl11b for T cell commitment. Nat. Immunol. *17*, 956–965.

Lee, T.V., Sethi, M.K., Leonardi, J., Rana, N.A., Buettner, F.F., Haltiwanger, R.S., Bakker, H., and Jafar-Nejad, H. (2013). Negative regulation of notch signaling by xylose. PLoS Genet. *9*, e1003547.

Lee, C., Sorensen, E.B., Lynch, T.R., and Kimble, J. (2016). C. elegans GLP-1/Notch activates transcription in a probability gradient across the germline stem cell pool. eLife *5*, e18370.

Li, L., Zhang, J.A., Dose, M., Kueh, H.Y., Mosadeghi, R., Gounari, F., and Rothenberg, E.V. (2013). A far downstream enhancer for murine Bcl11b controls its T-cell specific expression. Blood *122*, 902–911.

Li, Y., Bohm, C., Dodd, R., Chen, F., Qamar, S., Schmitt-Ulms, G., Fraser, P.E., and St George-Hyslop, P.H. (2014a). Structural biology of presenilin 1 complexes. Mol. Neurodegener. *9*, 59.

Li, Y., Lu, S.H., Tsai, C.J., Bohm, C., Qamar, S., Dodd, R.B., Meadows, W., Jeon, A., McLeod, A., Chen, F., et al. (2014b). Structural interactions between inhibitor and substrate docking sites give insight into mechanisms of human PS1 complexes. Structure *22*, 125–135.

Liefke, R., Oswald, F., Alvarado, C., Ferres-Marco, D., Mittler, G., Rodriguez, P., Dominguez, M., and Borggrefe, T. (2010). Histone demethylase KDM5A is an integral part of the core Notch-RBP-J repressor complex. Genes Dev. *24*, 590–601.

Lira-Navarrete, E., Valero-Gonzalez, J., Villanueva, R., Martinez-Julvez, M., Tejero, T., Merino, P., Panjikar, S., and Hurtado-Guerrero, R. (2011). Structural insights into the mechanism of protein O-fucosylation. PLoS One *6*, e25365.

Liu, F., and Posakony, J.W. (2012). Role of architecture in the function and specificity of two Notch-regulated transcriptional enhancer modules. PLoS Genet. *8*, e1002796.

Liu, F., and Posakony, J.W. (2014). An enhancer composed of interlocking submodules controls transcriptional autoregulation of suppressor of hairless. Dev. Cell *29*, 88–101.

Lu, P., Bai, X.C., Ma, D., Xie, T., Yan, C., Sun, L., Yang, G., Zhao, Y., Zhou, R., Scheres, S.H., et al. (2014). Three-dimensional structure of human gamma-secretase. Nature *512*, 166–170.

Luca, V.C., Jude, K.M., Pierce, N.W., Nachury, M.V., Fischer, S., and Garcia, K.C. (2015). Structural biology. Structural basis for Notch1 engagement of Delta-like 4. Science *347*, 847–853.

Luca, V.C., Kim, B.C., Ge, C., Kakuda, S., Wu, D., Roein-Peikar, M., Haltiwanger, R.S., Zhu, C., Ha, T., and Garcia, K.C. (2017). Notch-Jagged complex structure implicates a catch bond in tuning ligand sensitivity. Science *355*, 1320–1324.

Luty, W.H., Rodeberg, D., Parness, J., and Vyas, Y.M. (2007). Antiparallel segregation of notch components in the immunological synapse directs reciprocal signaling in allogeneic Th:DC conjugates. J. Immunol. *179*, 819–829.

Maier, D., Kurth, P., Schulz, A., Russell, A., Yuan, Z., Gruber, K., Kovall, R.A., and Preiss, A. (2011). Structural and functional analysis of the repressor complex in the Notch signaling pathway of *Drosophila melanogaster*. Mol. Biol. Cell *22*, 3242–3252.

McMillan, B.J., Schnute, B., Ohlenhard, N., Zimmerman, B., Miles, L., Beglova, N., Klein, T., and Blacklow, S.C. (2015). A tail of two sites: a bipartite mechanism for recognition of notch ligands by mind bomb E3 ligases. Mol. Cell *57*, 912–924.

Meloty-Kapella, L., Shergill, B., Kuon, J., Botvinick, E., and Weinmaster, G. (2012). Notch ligand endocytosis generates mechanical pulling force dependent on dynamin, epsins, and actin. Dev. Cell *22*, 1299–1312.

Morsut, L., Roybal, K.T., Xiong, X., Gordley, R.M., Coyle, S.M., Thomson, M., and Lim, W.A. (2016). Engineering customized cell sensing and response behaviors using synthetic notch receptors. Cell *164*, 780–791.

Mulligan, P., Yang, F., Di Stefano, L., Ji, J.Y., Ouyang, J., Nishikawa, J.L., Toiber, D., Kulkarni, M., Wang, Q., Najafi-Shoushtari, S.H., et al. (2011). A SIRT1-LSD1 corepressor complex regulates notch target gene expression and development. Mol. Cell *42*, 689–699.

Nellesen, D.T., Lai, E.C., and Posakony, J.W. (1999). Discrete enhancer elements mediate selective responsiveness of enhancer of split complex genes to common transcriptional activators. Dev. Biol. *213*, 33–53.

Oswald, F., Rodriguez, P., Giaimo, B.D., Antonello, Z.A., Mira, L., Mittler, G., Thiel, V.N., Collins, K.J., Tabaja, N., Cizelsky, W., et al. (2016). A phospho-dependent mechanism involving NCoR and KMT2D controls a permissive chromatin state at Notch target genes. Nucleic Acids Res. *44*, 4703–4720.

Parks, A.L., Klueg, K.M., Stout, J.R., and Muskavitch, M.A. (2000). Ligand endocytosis drives receptor dissociation and activation in the Notch pathway. Development *127*, 1373–1385.

Ramos, A.I., and Barolo, S. (2013). Low-affinity transcription factor binding sites shape morphogen responses and enhancer evolution. Philos. Trans. R. Soc. Lond. B Biol. Sci. *368*, 20130018.

Rothenberg, E.V. (2012). Transcriptional drivers of the T-cell lineage program. Curr. Opin. Immunol. *24*, 132–138.

Sannerud, R., Esselens, C., Ejsmont, P., Mattera, R., Rochin, L., Tharkeshwar, A.K., De Baets, G., De Wever, V., Habets, R., Baert, V., et al. (2016). Restricted location of PSEN2/gamma-secretase determines substrate specificity and generates an intracellular abeta pool. Cell *166*, 193–208.

Seo, D., Southard, K.M., Kim, J.W., Lee, H.J., Farlow, J., Lee, J.U., Litt, D.B., Haas, T., Alivisatos, A.P., Cheon, J., et al. (2016). A mechanogenetic toolkit for interrogating cell signaling in space and time. Cell *165*, 1507–1518.

Serneels, L., Dejaegere, T., Craessaerts, K., Horre, K., Jorissen, E., Tousseyn, T., Hebert, S., Coolen, M., Martens, G., Zwijsen, A., et al. (2005). Differential contribution of the three Aph1 genes to gamma-secretase activity in vivo. Proc. Natl. Acad. Sci. USA *102*, 1719–1724.

Sethi, M.K., Buettner, F.F., Krylov, V.B., Takeuchi, H., Nifantiev, N.E., Haltiwanger, R.S., Gerardy-Schahn, R., and Bakker, H. (2010). Identification of glycosyltransferase 8 family members as xylosyltransferases acting on O-glucosylated notch epidermal growth factor repeats. J. Biol. Chem. *285*, 1582–1586.

Sethi, M.K., Buettner, F.F., Ashikov, A., Krylov, V.B., Takeuchi, H., Nifantiev, N.E., Haltiwanger, R.S., Gerardy-Schahn, R., and Bakker, H. (2012). Molecular cloning of a xylosyltransferase that transfers the second xylose to O-glucosylated epidermal growth factor repeats of notch. J. Biol. Chem. *287*, 2739–2748.

Shaya, O., Binshtok, U., Hersch, M., Rivkin, D., Weinreb, S., Amir-Zilberstein, L., Khamaisi, B., Oppenheim, O., Desai, R.A., Goodyear, R.J., et al. (2017). Cell-cell contact area affects notch signaling and notch-dependent patterning. Dev. Cell *40*, 505–511.

Shergill, B., Meloty-Kapella, L., Musse, A.A., Weinmaster, G., and Botvinick, E. (2012). Optical tweezers studies on notch: single-molecule interaction strength is independent of ligand endocytosis. Dev. Cell *22*, 1313–1320.

Sherry, K.P., Johnson, S.E., Hatem, C.L., Majumdar, A., and Barrick, D. (2015). Effects of linker length and transient secondary structure elements in the intrinsically disordered notch RAM region on notch signaling. J. Mol. Biol. *427*, 3587–3597.

Sierra, O.L., Cheng, S.L., Loewy, A.P., Charlton-Kachigian, N., and Towler, D.A. (2004). MINT, the Msx2 interacting nuclear matrix target, enhances Runx2-dependent activation of the osteocalcin fibroblast growth factor response element. J. Biol. Chem. *279*, 32913–32923.

Skalska, L., Stojnic, R., Li, J., Fischer, B., Cerda-Moya, G., Sakai, H., Tajbakhsh, S., Russell, S., Adryan, B., and Bray, S.J. (2015). Chromatin signatures at Notch-regulated enhancers reveal large-scale changes in H3K56ac upon activation. EMBO J. *34*, 1889–1904.

Stanley, P., and Okajima, T. (2010). Roles of glycosylation in notch signaling. Curr. Top. Dev. Biol. *92*, 131–164.

Sun, L., Zhao, L., Yang, G., Yan, C., Zhou, R., Zhou, X., Xie, T., Zhao, Y., Wu, S., Li, X., et al. (2015). Structural basis of human gamma-secretase assembly. Proc. Natl. Acad. Sci. USA *112*, 6003–6008.

Swanson, C.I., Evans, N.C., and Barolo, S. (2010). Structural rules and complex regulatory circuitry constrain expression of a Notch- and EGFR-regulated eye enhancer. Dev. Cell *18*, 359–370.

Swanson, C.I., Schwimmer, D.B., and Barolo, S. (2011). Rapid evolutionary rewiring of a structurally constrained eye enhancer. Curr. Biol. *21*, 1186–1196.

Theodoris, C.V., Li, M., White, M.P., Liu, L., He, D., Pollard, K.S., Bruneau, B.G., and Srivastava, D. (2015). Human disease modeling reveals integrated transcriptional and epigenetic mechanisms of NOTCH1 haploinsufficiency. Cell *160*, 1072–1086.

Torella, R., Li, J., Kinrade, E., Cerda-Moya, G., Contreras, A.N., Foy, R., Stojnic, R., Glen, R.C., Kovall, R.A., Adryan, B., et al. (2014). A combination of computational and experimental approaches identifies DNA sequence constraints associated with target site binding specificity of the transcription factor CSL. Nucleic Acids Res. *42*, 10550–10563.

Troost, T., Schneider, M., and Klein, T. (2015). A re-examination of the selection of the sensory organ precursor of the bristle sensilla of *Drosophila melanogaster*. PLoS Genet. *11*, e1004911.

Tsuji, M., Shinkura, R., Kuroda, K., Yabe, D., and Honjo, T. (2007). Msx2-interacting nuclear target protein (Mint) deficiency reveals negative regulation of

early thymocyte differentiation by Notch/RBP-J signaling. Proc. Natl. Acad. Sci. USA *104*, 1610–1615.

Wang, X., and Ha, T. (2013). Defining single molecular forces required to activate integrin and notch signaling. Science *340*, 991–994.

Wang, H., Zou, J., Zhao, B., Johannsen, E., Ashworth, T., Wong, H., Pear, W.S., Schug, J., Blacklow, S.C., Arnett, K.L., et al. (2011). Genome-wide analysis reveals conserved and divergent features of Notch1/RBPJ binding in human and murine T-lymphoblastic leukemia cells. Proc. Natl. Acad. Sci. USA *108*, 14908–14913.

Wang, H., Zang, C., Taing, L., Arnett, K.L., Wong, Y.J., Pear, W.S., Blacklow, S.C., Liu, X.S., and Aster, J.C. (2014). NOTCH1-RBPJ complexes drive target gene expression through dynamic interactions with superenhancers. Proc. Natl. Acad. Sci. USA *111*, 705–710.

Weisshuhn, P.C., Handford, P.A., and Redfield, C. (2015a). (1)H, (13)C and (15)N assignments of EGF domains 4 to 7 of human Notch-1. Biomol. NMR Assign. *9*, 275–279.

Weisshuhn, P.C., Handford, P.A., and Redfield, C. (2015b). (1)H, (13)C and (15)N assignments of EGF domains 8-11 of human Notch-1. Biomol. NMR Assign. *9*, 375–379.

Weisshuhn, P.C., Sheppard, D., Taylor, P., Whiteman, P., Lea, S.M., Handford, P.A., and Redfield, C. (2016). Non-linear and flexible regions of the human Notch1 extracellular domain revealed by high-resolution structural studies. Structure *24*, 555–566.

Yabe, D., Fukuda, H., Aoki, M., Yamada, S., Takebayashi, S., Shinkura, R., Yamamoto, N., and Honjo, T. (2007). Generation of a conditional knockout allele for mammalian Spen protein Mint/SHARP. Genesis *45*, 300–306.

Yamamoto, S., Charng, W.L., Rana, N.A., Kakuda, S., Jaiswal, M., Bayat, V., Xiong, B., Zhang, K., Sandoval, H., David, G., et al. (2012). A mutation in EGF repeat-8 of Notch discriminates between Serrate/Jagged and Delta family ligands. Science *338*, 1229–1232.

Yashiro-Ohtani, Y., Wang, H., Zang, C., Arnett, K.L., Bailis, W., Ho, Y., Knoechel, B., Lanauze, C., Louis, L., Forsyth, K.S., et al. (2014). Long-range enhancer activity determines Myc sensitivity to Notch inhibitors in T cell leukemia. Proc. Natl. Acad. Sci. USA *111*, E4946–E4953.

Yatim, A., Benne, C., Sobhian, B., Laurent-Chabalier, S., Deas, O., Judde, J.G., Lelievre, J.D., Levy, Y., and Benkirane, M. (2012). NOTCH1 nuclear interactome reveals key regulators of its transcriptional activity and oncogenic function. Mol. Cell *48*, 445–458.

Yu, H., Takeuchi, M., LeBarron, J., Kantharia, J., London, E., Bakker, H., Haltiwanger, R.S., Li, H., and Takeuchi, H. (2015). Notch-modifying xylosyltransferase structures support an SNi-like retaining mechanism. Nat. Chem. Biol. *11*, 847–854.

Yu, H., Takeuchi, H., Takeuchi, M., Liu, Q., Kantharia, J., Haltiwanger, R.S., and Li, H. (2016). Structural analysis of Notch-regulating Rumi reveals basis for pathogenic mutations. Nat. Chem. Biol. *12*, 735–740.

Yuan, Z., Praxenthaler, H., Tabaja, N., Torella, R., Preiss, A., Maier, D., and Kovall, R.A. (2016). Structure and function of the Su(H)-hairless repressor complex, the major antagonist of notch signaling in drosophila melanogaster. PLoS Biol. *14*, e1002509.

Zhao, G., Liu, Z., Ilagan, M.X., and Kopan, R. (2010). Gamma-secretase composed of PS1/Pen2/Aph1a can cleave notch and amyloid precursor protein in the absence of nicastrin. J. Neurosci. *30*, 1648–1656.